https://doi.org/10.3311/PPch.42769

Periodica Polytechnica Chemical Engineering, 70(2), pp. 229–245, 2026

Enhanced Antimicrobial and Synergistic Antifungal Activity of *Centratherum anthelminticum* Seed Extract-Derived Silver Nanoparticles

Sadanand Yewale[1], Pradnya Deshpande[1], Vishal Gavande[2], Vasi Shaikh[1*]

[1] Department of Chemistry, Dr. Vishwanath Karad MIT World Peace University, Pune, Maharashtra - 411038, India
[2] Department of Materials Science and Engineering, Chair for Polymer Materials, Saarland University, Saarbrucken - 66123, Germany
[*] Corresponding author, e-mail: vasi.shaikh@mitwpu.edu.in

Received: 07 November 2025, Accepted: 17 April 2026, Published online: 27 May 2026

Abstract

With the increasing concern over antibiotic resistance and the side effects of synthetic drugs, there is a need for the development of novel and potent alternative bactericidal agents. Metallic nanoparticles, a promising alternative to antibiotics, target multiple biomolecules concurrently, making it difficult for bacteria to develop resistance against them. The present work reports the enhanced antimicrobial and synergistic antifungal activity of *Centratherum anthelminticum* (CA) seed-ethyl acetate (EA) extract-derived silver nanoparticles (AgNPs)—(CA-EA-AgNPs)—via biogenic synthesis. The CA-EA-AgNPs exhibited significantly enhanced antimicrobial activity against *Staphylococcus epidermidis*, *Staphylococcus aureus* (Gram-positive), *Proteus mirabilis*, and *Pseudomonas aeruginosa* (Gram-negative) bacteria compared to the crude CA-EA extract. CA-EA-AgNPs also demonstrated potent antifungal activity against the dandruff-causing fungus *Malassezia furfur* and displayed a synergistic effect when combined with ketoconazole, increasing the zone of inhibition from 15 mm (ketoconazole alone) and 11 mm (AgNPs alone) to 19 mm (combination). The synthesis of CA-EA-AgNPs was optimized by systematically varying parameters such as pH, temperature, reaction time, CA-EA extract concentration, and $AgNO_3$ concentration. The AgNPs were extensively characterized using UV-visible spectroscopy, dynamic light scattering, zeta potential, fourier transform infrared spectroscopy, X-ray diffraction, field emission scanning electron microscopy, transmission electron microscopy, and energy-dispersive X-ray analysis . To our knowledge, this research is the first to report the antifungal activity of *C. anthelminticum*-derived AgNPs against *Malassezia furfur*. The results highlight the potential of *C. anthelminticum* seed extract as a green resource for synthesizing AgNPs with promising applications in combating microbial infections, particularly skin and soft tissue infections.

Keywords

silver nanoparticles, green synthesis, *Centratherum anthelminticum*, antibacterial activity, antifungal activity, synergistic effect

1 Introduction

Nanotechnology is a rapidly advancing field with profound implications across diverse sectors, including agriculture, food science, and particularly biomedicine [1, 2]. Nanoparticles (NPs), defined as particulate matter with at least one dimension in the 1-100 nm range, exhibit unique physicochemical and biological properties – such as small size, large surface area-to-volume ratio, and quantum effects – distinct from their bulk counterparts [3, 4]. These characteristics have positioned them as viable candidates for innovative diagnostic and therapeutic uses, revolutionizing approaches to disease prevention and treatment [5]. Among various types of NPs, metallic nanoparticles derived from elements like silver, zinc, gold, and copper have garnered considerable focus due to their versatile biomedical applications [6]. However, conventional chemical and physical techniques for synthesizing these NPs often involve hazardous chemicals, high energy consumption, and cumbersome purification processes, posing environmental and biological risks [7–9]. These methods can result in the adsorption of harmful chemical compounds on the NP surface, limiting their biomedical utility [10].

Consequently, biogenic or "green" synthesis routes, employing biological entities such as plants, algae, fungi, or bacteria, have emerged as a cost-effective, eco-friendly, and sustainable alternative [11]. Plant-mediated synthesis is particularly advantageous due to the readily available and

Cite this article as: Yewale, S., Deshpande, P., Gavande, V., Shaikh, V. "Enhanced Antimicrobial and Synergistic Antifungal Activity of *Centratherum anthelminticum* Seed Extract-Derived Silver Nanoparticles", Periodica Polytechnica Chemical Engineering, 70(2), pp. 229–245, 2026. https://doi.org/10.3311/PPch.42769

diverse repertoire of phytochemicals (e.g., polyphenols, flavonoids, terpenoids, alkaloids) that can act as natural reducing, capping, and stabilizing agents, obviating the need for external toxic chemicals [12, 13]. This approach is generally simpler, faster, and more easily scalable compared to microbial synthesis, which can be time-consuming and require sterile conditions and elaborate culture maintenance [11]. Silver nanoparticles have been recognized for their remarkable antimicrobial properties for centuries and are among the most commercialized nanomaterials [14, 15]. They exhibit broad-spectrum activity against bacteria, fungi, and viruses, often at low concentrations where silver ions demonstrate good biocompatibility [16, 17]. The antimicrobial actions of AgNPs are diverse, involving cell membrane rupture, protein denaturation, DNA damage, and induction of oxidative stress [18, 19].

The integration of traditional medicinal knowledge with nanotechnology offers a promising avenue for developing novel bio-nano formulations [20]. Herbal medicines are gaining renewed interest due to their holistic approaches and perceived safety [21]. *Centratherum anthelminticum* (L.) Kuntze (syn. *Vernonia anthelmintica*), commonly referred to as kalijiri or somraj, is a member of the Asteraceae family. Its seeds have a long history of use in traditional medicine for treating various ailments, including skin diseases, fever, parasitic infections, and diuretic activity [22, 23], which are attributed to its rich phytochemical profile, including flavonoids, sterols, and sesquiterpene lactones [24].

Although the green synthesis of silver nanoparticles using various plant extracts has been widely reported, studies predominantly focus on aqueous extracts [25, 26]. The present study employs ethyl acetate, a moderately polar, low-toxicity, and low-boiling solvent with environmental advantages. Owing to its intermediate polarity, ethyl acetate is hypothesized to selectively extract both lipophilic and hydrophilic constituents from plant material, including secondary metabolites such as phenolics, polyphenols, flavonoids, alkaloids, certain terpenoids, and antioxidants, while largely excluding sugars, salts, and chlorophyll when compared to other solvents [27]. Additionally, its compatibility with cell-based assays makes it particularly suitable for biological investigations.

The present work demonstrates its uniqueness through the use of ethyl acetate as the extraction solvent for *Centratherum anthelminticum* seeds, a solvent system that has been rarely explored, if at all, for this plant species. Most of the previously reported studies have predominantly utilized aqueous extracts of *C. anthelminticum* plant parts other than seeds, with a primary focus on antibacterial activity. In contrast, the present work reports the biological activity of the seed extract of *C. anthelminticum*. The current study also expands its scope to include synthesis of silver nanoparticles mediated by the above extract and investigates both antibacterial and antifungal activity. Furthermore, this work represents a novel attempt to evaluate the synergistic effect of the biogenically synthesized nanoparticles with a commercially available ketoconazole formulation, aiming to enhance its antifungal efficacy. The combined approach provides new insights into the potential of plant-mediated nano-silver systems as effective adjuvants in antifungal therapy. To our knowledge, no prior studies have reported the biogenic synthesis of AgNPs using seed extracts of *Centratherum anthelminticum*, specifically the ethyl acetate fraction, and investigated their antimicrobial and synergistic antifungal potential.

Comprehensive reviews have highlighted the use of a wide range of plant species such as *Ocimum sanctum*, *Curcuma longa*, *Azadirachta indica*, *Camellia sinensis*, and many others for AgNP fabrication, with detailed discussions on how extract composition, pH, temperature, and reaction time influence particle size, shape, stability, and functionality [28, 29]. Recent systematic analyses also emphasize biomedical applications, especially antimicrobial and antioxidant activities, underscoring the importance of phytochemical profiles in tuning biological efficacy. Experimental studies on specific plants, such as *Withania coagulans*, report synthesis of ~37 nm AgNPs exhibiting strong inhibitory effects against *Klebsiella pneumoniae* and *Salmonella typhi*, alongside acceptable biocompatibility profiles [30]. Similarly, phytosynthesis from *Mentha* (mint) leaf extracts shows efficient AgNP formation with pronounced antimicrobial and pharmacological properties [31]. The choice of plant source markedly impacts nanoparticle characteristics; for example, *Coleus aromaticus* produced ~44 nm AgNPs with significant bactericidal activity toward *Bacillus subtilis* and *Klebsiella planticola* [32], *Magnolia alba* leaves aqueous extract produced slightly larger-sized nanoparticles (~40 nm) [26], while the ethyl acetate extract of the *Urtica diocia* leaves produced smaller-sized (~19 nm) nanoparticles [33]. Jaison et al. reported the green synthesis of nanoparticles from the plant extracts of the Asteraceae family, including the ethyl acetate extract of *Blumea balsamifera*, which produced silver nanoparticles of size ranging 30-55 nm [34], while the present study reported *Centratherum anthelminticum* seed-ethyl acetate (EA) extract-derived silver nanoparticles (CA-EA-AgNPs) size ranging 11-17 nm,

reinforcing how varying phytochemical matrices influence bioactivity. Across studies, color change (typically to brown) and surface plasmon resonance peaks in UV–Vis spectra remain consistent indicators of AgNP formation, while advanced characterizations (X-ray diffraction XRD, Fourier transform infrared spectroscopy FTIR, field emission scanning electron microscopy FESEM) confirm crystalline structures and capping interactions [28]. These collective findings from both experimental research and recent reviews consistently demonstrate that plant-mediated AgNP synthesis not only enables tunable physicochemical features but also enhances functional properties for antimicrobial, antioxidant, and catalytic applications, offering important insights for further optimization and translational research [28]. This study, therefore, is aimed to (i) synthesize AgNPs using an ethyl acetate extract of CA seeds; (ii) optimize the synthesis parameters; (iii) characterize the synthesized AgNPs using various analytical techniques; (iv) evaluate their antimicrobial activity (against clinically relevant bacteria mentioned above); and (v) assess their antifungal activity against *Malassezia furfur*, including a synergistic study with ketoconazole. This research explores the potential of CA-EA-AgNPs as a novel antimicrobial agent, particularly for topical applications.

2 Materials and methods

2.1 Materials

Soybean casein digest agar (SCDA), soybean casein digest medium (SCDB), yeast peptone dextrose agar (YEPD), yeast peptone dextrose broth (YEPDB), silver nitrate (purity > 99.90%), and streptomycin sulfate were procured from HiMedia Laboratories Pvt. Ltd., Mumbai, India. Methanol (HPLC grade, purity > 99%), aqueous ammonia (25%), n-hexane, chloroform, ethyl acetate and acetone (all analytical grade) were purchased from Merck, India. Bacterial strains: *Staphylococcus epidermidis* (MTCC 2639), *Staphylococcus aureus* (MTCC 9542), *Pseudomonas aeruginosa* (MTCC 1934), *Proteus mirabilis* (MTCC 9242), and the fungal strain *Malassezia furfur* (MTCC 1765) were obtained from the Microbial Type Culture Collection and Gene Bank (MTCC), Chandigarh, India. Commercial antidandruff shampoo (containing 2% w/v ketoconazole) was purchased from a local pharmacy. Deionized (DI) water was used for all solution preparations and dilutions. *Centratherum anthelminticum* seeds were purchased from a local herbal store in Pune, India, and dried in the shed and cleaned before use. Solvents - hexane, chloroform, ethyl acetate, acetone, ethanol, and methanol (Merck India) - were used as received.

2.2 Methods

2.2.1 Plant material authentication and extract preparation

The CA seeds were taxonomically identified and authenticated as per the standard protocol and were cleaned, shade-dried, and crushed into a fine powder before use. Powder microscopy revealed abundant uniseriate trichomes (166.7-194.5 µm in length). The ground tissue was multilayered and comprised of thick-walled, compactly arranged parenchymatous cells. Sclerenchymatous elements included thin-walled fibers, pitted tracheids from the hilum furrow, and elongated and rectangular stone cells (sclereids) with a lumen of variable width (appearing both broad and narrow). Fig. 1 represents the photomicrographs of the CA plant, CA seeds, and powdered CA seeds.

The powdered material was subjected to successive Soxhlet extraction for a predetermined time with solvents in the order of increasing polarity: *n*-hexane, chloroform, ethyl acetate, acetone, ethanol, water, and methanol. Each of the above extracts was subjected to preliminary screening for phytochemical content and antimicrobial activity. From among the above extracts, the EA extract was chosen for nanoparticle synthesis based on the above preliminary results (i.e., phytochemical content and highest antimicrobial activity). The CA-EA extract was eventually filtered, concentrated, and dried under reduced pressure, and the resulting viscous residue was stored at 4 °C in sealed sample tubes for further use. A reported extraction procedure with minor modifications was adopted for the same [16].

2.2.2 Phytochemical profiling of *Centratherum anthelminticum* seed-ethyl acetate extract

Determination of total polyphenolic content

Total polyphenolic content (TPC) was assessed utilizing the Folin-Ciocalteu technique as reported in literature with minor modifications [35]. Gallic acid was used as a standard, and TPC was expressed as mg of gallic acid

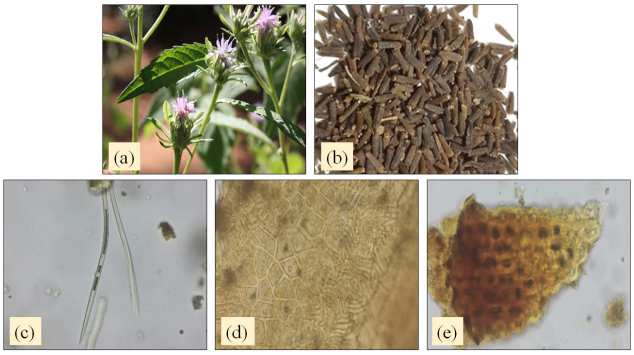

Fig. 1 (a) CA plant, (b) CA seeds, (c) uniseriate trichomes, and photomicrographs of (d) stone cells and (e) sclerenchymatous cells

equivalents per gram of dry extract (mg GAE/g DW). The calibration curve for gallic acid is represented by using the Eq. (1):

$$y = 0.007x - 0.0264\left(R^2 = 0.9941\right) \quad (1)$$

Determination of total flavonoid content

Total flavonoid content (TFC) was determined using the aluminum chloride colorimetric method with minor modifications to the method described by Formagio et al. [36]. Quercetin served as the standard, and TFC was quantified as mg of quercetin equivalents per gram of dry extract (mg QE/gDW). The calibration curve for quercetin is represented by the Eq. (2):

$$y = 0.0085x - 0.0096\left(R^2 = 0.9933\right) \quad (2)$$

Determination of reducing power capacity

The reducing power of the CA-EA extract was determined according to the method described by Bhalodia et al. [37], where ascorbic acid served as the standard and reducing power was quantified as mg of ascorbic acid equivalents per gram of dry extract (mg ASE/g DW). The Eq. (3)

$$y = 0.019x - 0.1133\left(R^2 = 0.9937\right) \quad (3)$$

represents the calibration curve for ascorbic acid.

Experimental observations for TPC, TFC, and the reducing power capacity of the CA-EA extract are presented in Table 1. Fig. 2 represents the standard curves for (a) gallic acid, (b) quercetin, and (c) ascorbic acid based on values from Table 1.

2.2.3 Biogenic synthesis of silver nanoparticles

A stock solution of CA-EA extract (10 mg/mL) was prepared in methanol and diluted with DI water before use. An $AgNO_3$ stock solution (100 mM) was prepared using DI water and stored in an amber-colored bottle. The synthesis of CA-EA-AgNPs was optimized by systematically altering one parameter at a time while maintaining others constant, as discussed in the next section.

Table 1 Experimental observations for TPC, TFC, and reducing power capacity

Conc. (µg/mL)	Absorbance (Gallic acid) TPC	Absorbance (Quercetin) TFC	Absorbance (Ascorbic acid) Reducing power capacity
20	0.122	0.15	0.237
40	0.257	0.323	0.635
60	0.372	0.517	1.095
80	0.513	0.697	1.442
100	0.689	0.812	1.738

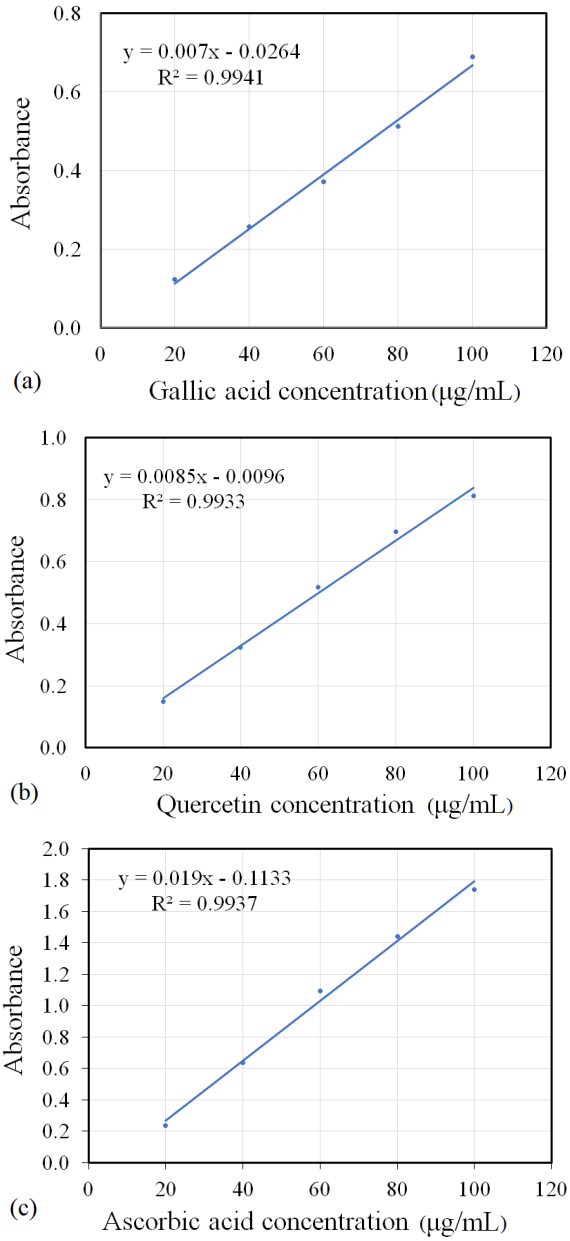

Fig. 2 The standard curves for (a) gallic acid, (b) quercetin, and (c) ascorbic acid

2.2.4 Optimizing factors for the biogenic synthesis of *Centratherum anthelminticum* seed-ethyl acetate extract-derived silver nanoparticles

Effect of Centratherum anthelminticum seed-ethyl acetate extract concentration

CA-EA extract concentrations from 25 to 2000 µg/mL were tested on biogenic synthesis. AgNPs were synthesized as described in Section 2.2.3. The nanoparticle solution was examined by UV-visible spectroscopy

(Shimadzu UV-1900, Japan) at 300-600 nm and absorbance at 0.1–4. For silver nanoparticle synthesis, CA-EA extract concentration was established by UV absorbance or surface plasmon resonance (SPR) intensity [16].

Effect of pH and temperature
The effect of pH was assessed over a pH range of 6 to 11 as per the literature method. The synthesis was attempted at pH 6, 7, 8, 9, 10, and 11 [38]. The effect of temperature was observed over the temperature range of 30 to 90 °C in the interval of 30, 50, 70, and 90 °C in the dark for 1 h [39]. AgNPs formed in both cases were characterized with UV-visible spectroscopy as described above.

Effect of silver nitrate concentration
The effect of silver nitrate concentration on biogenic synthesis of AgNPs was studied over a range of 1 mM to 50 mM, and the optimum concentration was finalized based on the UV-Visible absorbance intensity [40].

Effect of time
The time required for the nanoparticle synthesis at various temperatures was studied, and based on the stable absorbance intensity, the optimum time for the nanoparticle synthesis was set [41].

For a typical optimized synthesis, 10 mL of aqueous CA-EA extract (1000 µg/mL) was mixed with 90 mL of aqueous $AgNO_3$ solution (10 mM), adjusting the pH at 10 using aq. ammonia (2.5%) and maintaining it at 90 °C for 45 min in the dark with constant stirring at 150 rpm. A color transition from pale yellow to reddish-brown signifying AgNP formation was monitored using a UV-Vis spectrophotometer. The resulting CA-EA-AgNP suspension was centrifuged (10,000 rpm) at 4 °C, washed repeatedly with DI water, and re-dispersed in DI water for further characterization and bioassays, or freeze-dried (Lyophilizer, Labconco, USA) for solid-state characterization (XRD, FTIR, FESEM) and stored at 4 °C in the dark [42].

2.2.5 Characterization of *Centratherum anthelminticum* seed-ethyl acetate extract-derived silver nanoparticles
UV-Visible spectroscopy
The bioreduction of Ag^+ ions was assessed by studying the UV-Visible (UV-Vis) spectra of the reaction mixture at different time intervals between 300-600 nm using a (Shimadzu UV-1900, Japan) spectrophotometer at RT using DI water as a blank and compared with *C. anthelminticum* extract (1000 µg/mL) and silver nitrate solution [43].

Fourier transform infrared spectroscopy
FTIR spectra of the KBr pellets of CA-EA-AgNPs were studied using a (Thermo Scientific Nicolet iS5 FTIR spectrometer, USA) over the range of 4000-500 cm^{-1} and compared against CA-EA extract (1000 µg/mL) [44].

X-ray diffraction analysis
The crystalline nature of the lyophilized CA-EA-AgNPs was analyzed using an X-ray diffractometer (Panalytical Empyrean, Netherlands) with Cu Kα radiation (λ = 1.5406 Å) at 40 kV and 30 mA. Data were collected over a 2θ range of 30°-90° with a scan rate of 0.02°/s [45].

Field emission scanning electron microscopy, energy-dispersive X-ray and transmission electron microscopy analysis
The morphology and elemental composition of CA-EA-AgNPs were examined using a Nova Nano FESEM 450 (Field Electron and Ion Company (FEI) Nova NanoSEM 450, USA) instrument coupled with an EDAX detector. The size, shape, and morphology of the silver nanoparticles were determined by TEM analysis. A sample thin film was created on a copper grid that was coated with carbon, dried, and then sputter-coated with a thin layer of gold under vacuum before imaging [46, 47].

Dynamic light scattering and zeta potential analysis
Hydrodynamic particle size distribution, polydispersity index (PDI), and zeta potential (ζ) of the CA-EA-AgNP suspension (diluted in DI water and sonicated for 5 min) were determined using a Zetasizer Nano ZS (Malvern Instruments, UK) at 25 °C with a scattering angle of 90° [7].

2.2.6 Antimicrobial activity assessment
The agar well diffusion method was utilized for assessing both antimicrobial and antifungal activity [48]. Bacterial inocula were prepared from pure cultures using SCDB, while fungal inocula were prepared from pure cultures using YEPDB. Antibacterial and antifungal activity was assessed using the SCDB and YEPDB, respectively.

Preparation of inocula
Bacterial strains (*S. aureus*, *S. epidermidis*, *P. aeruginosa*, *P. mirabilis*) were revived by inoculating into SCDB and incubating at 37 °C for 18-24 h. The fungal strain (*M. furfur*) was revived in YEPDB and incubated at 30 °C for 48-72 h as per the reported procedures [49–52].

Agar well diffusion assay

Antimicrobial and antifungal activity was evaluated by the agar well diffusion method using SCDA and YEPD agar plates, respectively, having wells with a diameter of 8 mm created in the agar using a sterile cork borer [48].

2.2.7 Statistical analysis

All the experiments were performed in triplicate ($n = 3$), and the results are expressed as mean ± standard deviation (SD). Statistical analysis was conducted using one-way analysis of variance (ANOVA) to evaluate differences among groups, and the differences were considered statistically significant at $p < 0.05$.

3 Results and discussion

The present study is aimed at the successive extraction of *C. anthelminticum* seeds using various solvents with varying polarity, their antibacterial efficacy, and the biogenic synthesis of silver nanoparticles using the above extracts. All the above extracts were checked for their antibacterial activity. The extract showing promising results, i.e., the highest antibacterial activity, was chosen for further study – i.e., biogenic synthesis of silver nanoparticles and their antimicrobial and antifungal study on various microbial and fungal strains. As discussed above in Section 2.2.1, the ethyl acetate extract exhibited the most promising results in terms of highest antibacterial activity; hence, the ethyl acetate extract of *C. anthelminticum* was chosen to synthesize the silver nanoparticles (CA-EA-AgNPs) biogenically.

3.1 Phytochemical analysis of *Centratherum anthelminticum* seed ethyl acetate extract

The ethyl acetate extract of *C. anthelminticum* seeds (CA-EA) was analyzed for its total polyphenolic content, total flavonoid content, and reducing power capacity, as these phytoconstituents are primarily responsible for the reduction of Ag^+ ions and stabilization of AgNPs [12]. The results are summarized in Table 2. The CA-EA extract exhibited a significant TPC of 124.63 ± 0.8 mg GAE/g DW and TFC of 28.78 ± 0.3 mg QE/g DW. The reducing power was found to be 94.02 ± 0.6 mg ASE/g DW. These results indicate a substantial presence of phenolic and flavonoid compounds, which possess hydroxyl and carbonyl groups capable of donating electrons for the reduction of Ag^+ to Ag^0 and subsequently capping the formed AgNPs to prevent aggregation [53]. The majority of phytochemicals recovered in polar solvents play a key role in the preparation of nanoparticles [54].

3.2 Optimization of *Centratherum anthelminticum* seed-ethyl acetate extract-derived silver nanoparticle synthesis

The formation of biogenically synthesized nanoparticles and their particle size is strongly influenced by extract concentration, reaction time, pH, and temperature, which collectively govern the reduction kinetics, nucleation rate, and capping efficiency of phytochemicals. The synthesis of CA-EA-AgNPs in the present study was optimized by monitoring the maximum SPR peak intensity using UV-Vis spectroscopy. Upon addition of CA-EA extract to the $AgNO_3$ solution under optimized conditions, a gradual color change from pale yellow to reddish-brown was observed within 10-15 min, intensifying over 45 min (Fig. 3(a)). This color change is a hallmark of AgNP formation due to the excitation of SPR [55]. The UV-Vis spectrum of the synthesized CA-EA-AgNPs displayed a characteristic SPR peak at 434 nm (Fig. 3(b)), consistent with previously reported AgNPs [17]. The CA-EA extract alone and the $AgNO_3$ solution alone did not show any absorbance peak in this region (Fig. 3(b) insets).

3.2.1 Effect of synthesis parameters

The optimization results are summarized in Table 3 and illustrated in Fig. 4.

Concentration of ethyl acetate extract of Centratherum anthelminticum seeds

The SPR intensity increased with extract concentration up to 1000 µg/mL, beyond which it slightly decreased or plateaued, possibly due to excessive phytochemicals causing aggregation or light scattering [56] (Fig. 4(a)).

Table 2 Phytochemical analysis of ethyl acetate extract of *C. anthelminticum* seeds

S. N.	Phytochemical estimation	Content (mg/g)	Content (%)
1	Total polyphenol content	124. 63 ± 0.8 mg GAE/g	12.09 ± 0.08
2	Total flavonoid content	28.78 ± 0.3 mg QE/g	2.76 ± 0.04
3	Reducing power capacity	94.02 ± 0.6 mg ASE/g	8.81 ± 0.06

*GAE = gallic acid equivalent, QE = quercetin equivalent, ASE = ascorbic acid equivalent

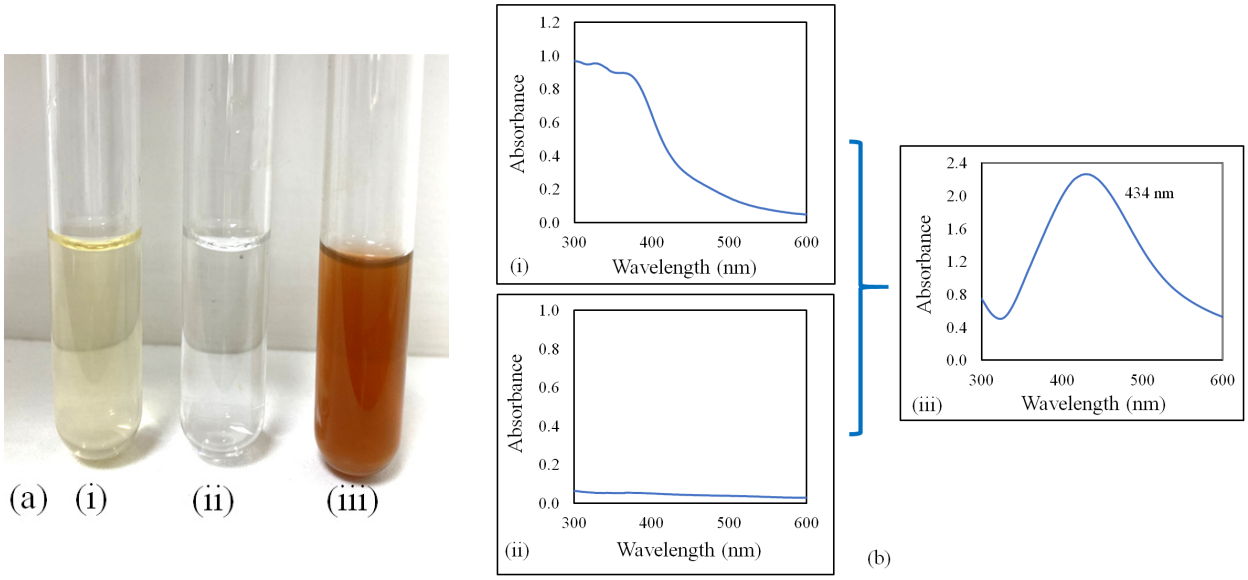

Fig. 3 (a) Visual confirmation of CA-EA-AgNPs synthesis: (i) CA-EA extract, (ii) $AgNO_3$ solution, (iii) CA-EA-AgNPs suspension after 45 min. (b) UV-Vis absorption spectrum of CA-EA-AgNPs showing SPR peak at 434 nm. Insets: UV-Vis spectra of CA-EA extract (1000 µg/mL) and $AgNO_3$ solution (10 mM).

Table 3 Optimized parameters for the biogenic synthesis of CA-EA-AgNPs

Parameters	Experimental values	Optimum value
CA-EA extract concentration (µg/mL)	25, 50, 100, 200, 300, 400,500, 1000, 2000	1000
$AgNO_3$ concentration (mM)	1, 2, 5, 10, 15, 20, 30, 40, 50	10
Reaction pH	6, 7, 8, 9, 10, 11	10
Reaction time (min)	5, 10, 15, 20, 30, 45, 60	45
Reaction temperature (°C)	30, 50, 70, 90	90

$AgNO_3$ concentration

The SPR intensity increased up to 10 mM $AgNO_3$, then decreased at higher concentrations, likely due to incomplete reduction or rapid aggregation of NPs [57] (Fig. 4(b)).

pH

The SPR intensity was maximal at pH 10. Alkaline pH facilitates the deprotonation of hydroxyl groups in phytochemicals, enhancing their reducing capacity. A similar effect of pH on the synthesis of silver nanoparticles utilizing the extract of *Pometia pinnata* (Matoa) leaves as a reducing agent has been reported [58] (Fig. 4(c)).

Temperature

The SPR intensity increased with temperature, with 90 °C being optimal, indicating that higher temperatures accelerate the reaction rate [59] (Fig. 4(d)).

Reaction time

The SPR peak intensity increased steadily with time, reaching a maximum at 45 min at 90 °C, after which it stabilized, indicating completion of the reaction (Fig. 4(e)). Optimization at room temperature (25 °C) required a much longer time (approx. 240 min).

3.3 Characterization of *Centratherum anthelminticum* seed-ethyl acetate extract-derived silver nanoparticles

3.3.1 Polydispersity index and zeta potential

The analysis using dynamic light scattering (DLS) revealed an average hydrodynamic diameter of 46.58 nm for the CA-EA-AgNPs, accompanied by a PDI of 0.503 (Fig. 5(a)). A low PDI value of 0.503 suggests a relatively moderate and homogenous dispersion [3]. The zeta potential was −22.0 mV (Fig. 5(b)), indicating moderate colloidal stability due to electrostatic repulsion between the negatively charged nanoparticles. The negative charge likely arises from the ionization of hydroxyl or carboxyl groups of capping phytochemicals on the NP surface [55]. Furthermore, the hydrodynamic size might be influenced by the phytochemicals in the seed extract. For cells to absorb, nanoparticles smaller than 150 nm are sufficient in size [5, 60]. The higher the negative or positive ζ-potential, the higher the stability,

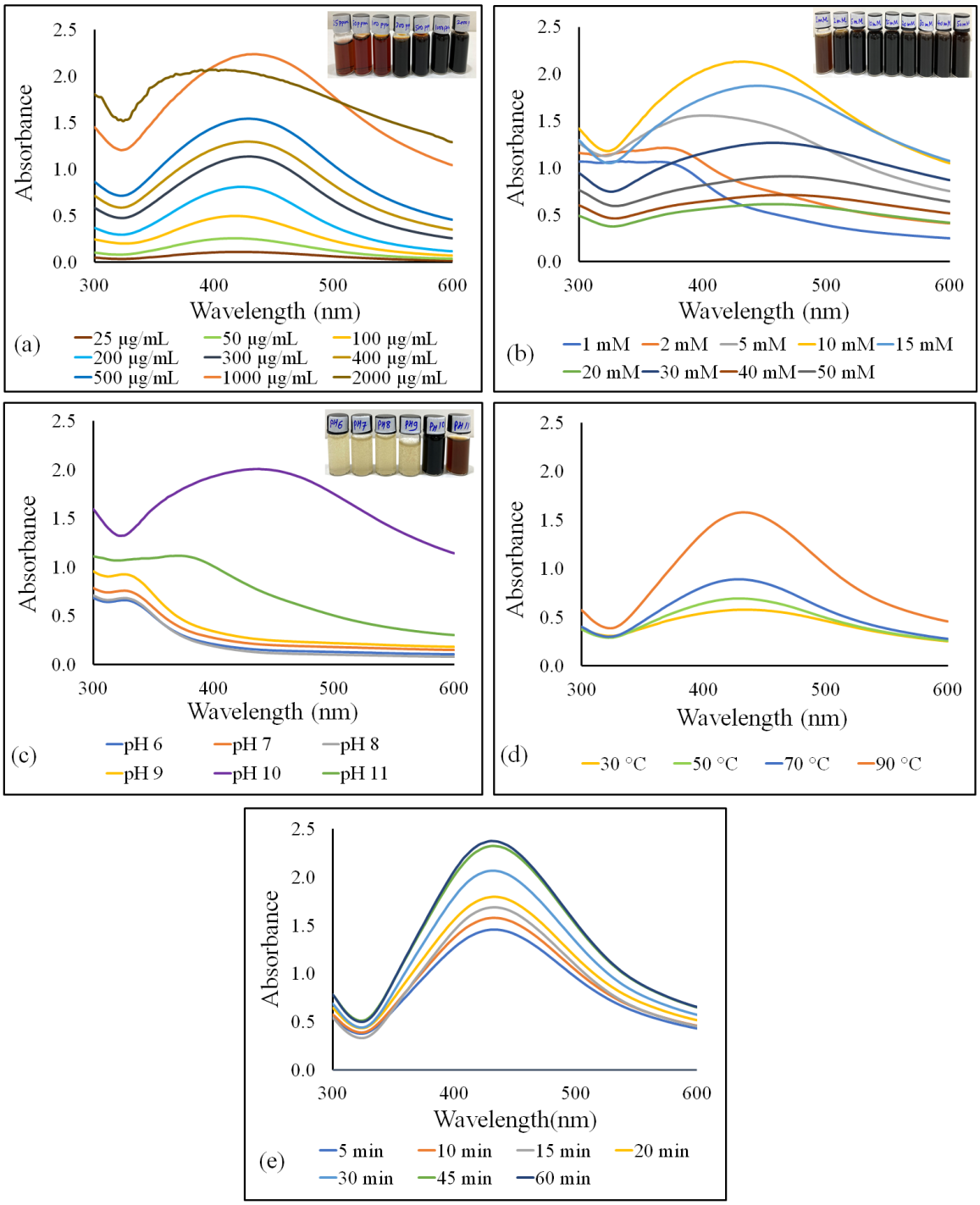

Fig. 4 Optimization of CA-EA-AgNPs synthesis parameters monitored by UV-Vis spectroscopy. Effect of (a) CA-EA extract concentration, (b) $AgNO_3$ concentration, (c) reaction pH, (d) reaction temperature, and (e) reaction time at 90 °C on SPR intensity.

the better the colloidal properties due to electrostatic repulsion, and the higher the dispersity [61]. The ζ-potential of CA-EA-AgNPs was negative, suggesting that negatively charged functional groups from the plant extract contribute to the colloidal stability of the AgNPs [62].

3.3.2 FTIR analysis

FTIR spectroscopy was employed to determine the secondary metabolites that play a role in the reduction and capping of CA-EA-AgNPs. The FTIR spectrum of the *C. anthelminticum* seed extract showed prominent peaks at 3339, 2933, 2250, 1720, 1352, 1138, 941, and 637 cm^{-1}

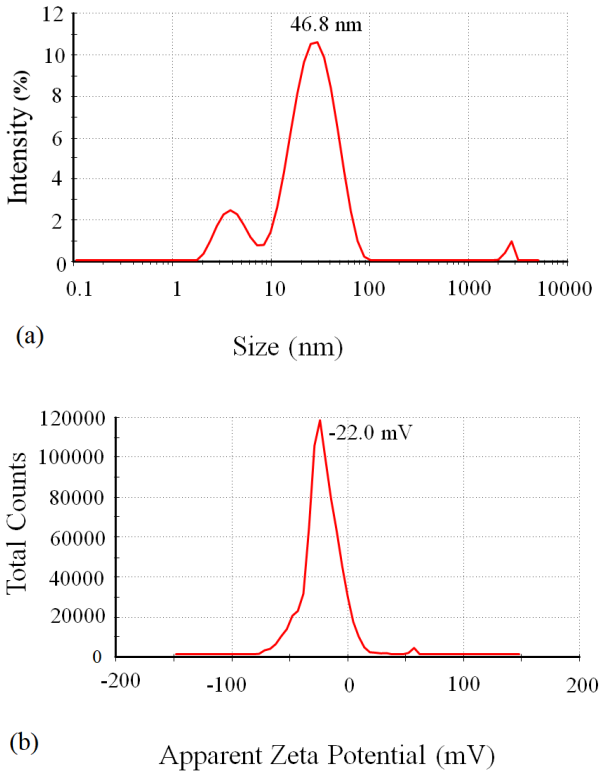

Fig. 5 (a) Dynamic light scattering analysis showing hydrodynamic size distribution of CA-EA-AgNPs, (b) zeta potential analysis showing colloidal stability of nanoparticles

(Fig. 6(a)). The FTIR spectrum of CA-EA-AgNPs displayed significant absorption peaks at 3741, 3314, 2348, 1653, 1424, 1286, 1015, and 912 cm^{-1}, indicating the presence of phytoconstituents serving as capping agents [63, 64] (Fig. 6(b)). The FTIR spectra of the *C. anthelminticum* seed extract corresponding to CA-EA-AgNPs showed substantial and small changes in the peaks,

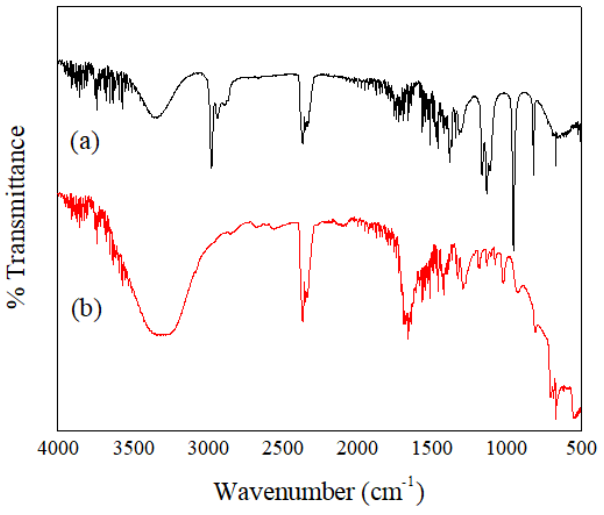

Fig. 6 FTIR spectra of (a) *C. anthelminticum* ethyl acetate (CA-EA) extract and (b) CA-EA-AgNPs

possibly attributable to the reduction, capping, and stabilization of the synthesized nanoparticles [65]. The peak at 3339 cm^{-1} shifts to a lower wavelength of 3314 cm^{-1} due to O–H or N–H stretching of phenolic chemicals in the seed extract [66]. The absorption peak at 2933 cm^{-1} is attributed to the C–H stretching of phenolic substances, organic acids, alkanes, and aldehydes [67]. The band at 2348 cm^{-1} may be due to the presence of phosphine [68]. The band at 1720 cm^{-1} shifted to a lower wavelength of 1653 cm^{-1} showing the involvement of alkenyl or aromatic C=C stretch and C=O amide group stretching [64, 65]; the band at 1424 cm^{-1} showed the presence of secondary amines; and the band shifting to higher frequency at 1286 cm^{-1}, 1015 cm^{-1}, 912 cm^{-1} and 664 cm^{-1} may be attributed to various phytochemicals such as polyphenols, glycosides, flavonoids, triterpenoids, alkaloids, etc. present in the extract responsible for the bio-reduction and formation of CA-EA-AgNPs nanoparticles [61, 66].

3.3.3 XRD analysis

The biosynthesized CA-EA-AgNPs exhibit five prominent X-ray diffraction peaks at 2θ = 38.59, 44.38, 64.78, 77.64, and 81.02° (Fig. 7). These prominent peaks in the spectrum, which correspond to the (111), (200), (220), (311), and (222) planes, respectively, indicate the patterns of the cubic close-packed (ccp), also called face-centric cubic (fcc), and crystalline structure of the biosynthesized AgNPs [69–71]. The XRD peak patterns are substantially influenced by the size of the nanoparticles. The presence of reducing agents in the extract plays a crucial role in stabilizing AgNPs and consequently contributes to the crystalline structure of AgNPs, which has been thoroughly examined (sharpness of the peaks) in numerous biosynthesized nanoparticles [72].

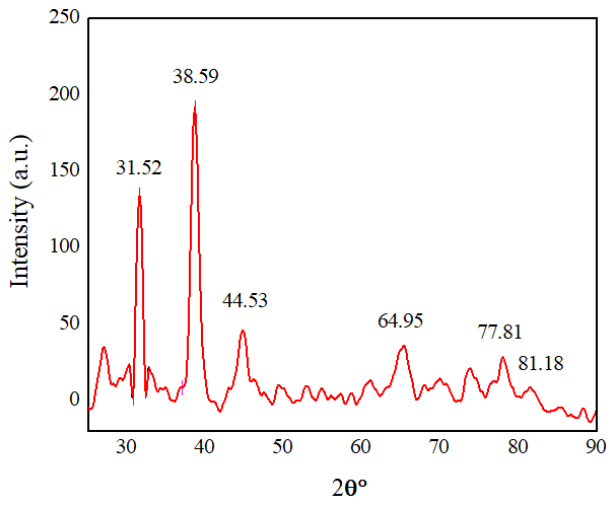

Fig. 7 X-ray diffraction pattern of CA-EA-AgNPs

3.3.4 FESEM, TEM and EDAX analysis

FESEM was used to investigate the morphology of biogenically synthesized CA-EA-AgNPs. The synthesized CA-EA-AgNPs were discovered to be irregularly granulated or spherical, somewhat polymorphic, and well-dispersed, although some aggregation was observed, likely due to the involvement of multiple biomolecules acting simultaneously as reducing and capping agents at different rates, leading to non-uniform nucleation, anisotropic growth due to non-selective capping, and polymorphic particle formation [73] (Fig. 8(a)). The spherical shape of nanoparticles is due to the reducing agent present in the seed extract of *C. anthelminticum* [74, 75]. Microscopic examination utilizing a scanning electron microscope revealed that the CA-EA-AgNPs exhibited uniform distribution. The size of CA-EA-AgNPs from FESEM analysis was found to be in the range of 16–27 nm, which is smaller than the hydrodynamic diameter from DLS. The hydrodynamic size (46.58 nm) is typically larger than that observed by FESEM (16–27 nm) due to the silver core with plant-derived capping agents and bound solvent molecules (hydration shell) on its surface, creating a soft organic corona increasing hydrodynamic radius, while FESEM measures the dry, solid core in a high-vacuum environment [76, 77]. Furthermore, the substantial aggregation of the biosynthesized AgNPs was presumably caused by the dehydration exerted during the preparation of samples for FESEM examination [78]. The TEM micrographs of the CA-EA-AgNPs are shown in Fig. 8(b). The typical diameter of the nanoparticles was found to be between 11-17 nm. It showed a nearly spherical shape morphology of the AgNPs, and they are well distributed and distanced from each other.

EDAX analysis confirmed the presence of elemental silver as the major constituent, with a strong signal at ~3 keV, characteristic of metallic silver [79] (Fig. 8(c)). Other signals for C, O, and N were also detected, likely originating from the phytochemical capping of the AgNPs, which plays an essential role in the reduction and stability of biosynthesized CA-EA-AgNPs [80]. The Al signal might be from the sample stub or minor impurities, and Au from the sputter coating [81]. Supported by EDAX analysis, it can be corroborated that there is a consistency in the distribution of silver elements in biogenically produced silver nanoparticles [82].

3.4 Antimicrobial activity

The antibacterial activity of the CA-EA extracts and biosynthesized CA-EA-AgNPs was checked by the agar well diffusion method against *S. aureus* and *S. epidermidis*

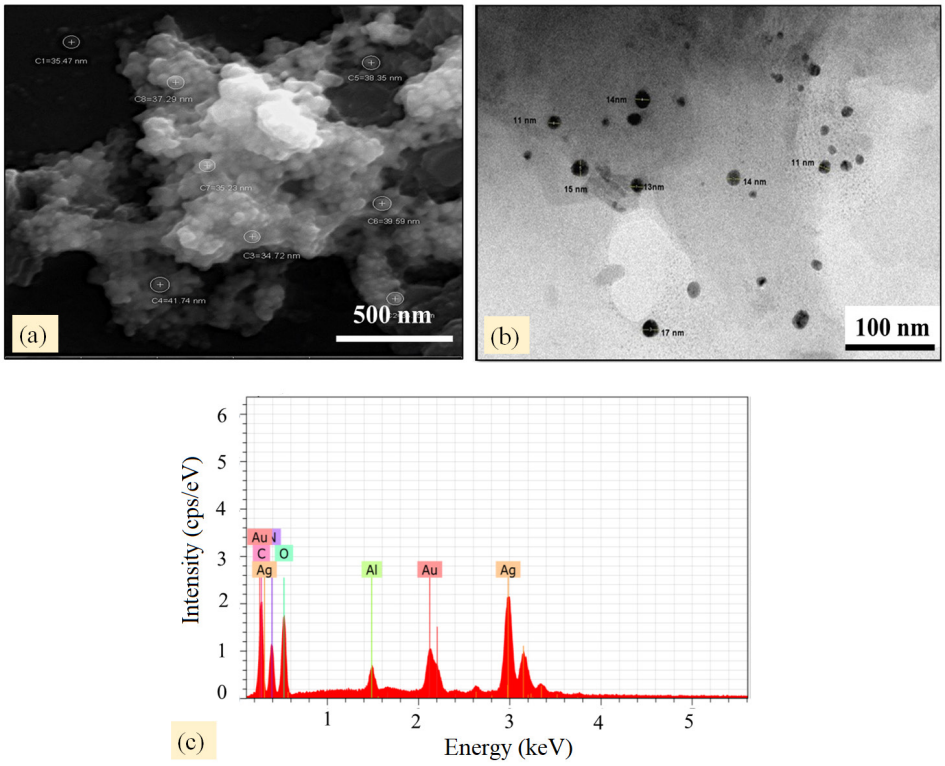

Fig. 8 (a) Field emission scanning electron microscopy image of CA-EA-AgNPs showing spherical morphology and size, (b) transmission electron microscopy images of CA-EA-AgNPs, (c) energy-dispersive X-ray spectrum confirming the elemental composition of CA-EA-AgNPs

(Gram-positive) and *P. aeruginosa* and *P. mirabilis* (Gram-negative) bacteria, as shown in Fig. 9. CA-EA-AgNPs demonstrated significantly greater antibacterial efficacy against all examined microorganisms relative to the CA-EA extract alone, as indicated by the zone of inhibition. The results, expressed as zones of inhibition (ZOI), are presented in Table 4 and graphically in Fig. 10.

The antibacterial activity of CA-EA-AgNPs was notably superior to that of the CA-EA extract at both concentrations tested (1000 µg/mL and 2000 µg/mL), as detailed in Table 4. Against the Gram-positive bacterium *S. aureus*, the CA-EA-AgNPs exhibited a zone of inhibition (ZOI) of 15.00 ± 1.00 mm, which was greater than the 9.67 ± 0.6 mm and 10.67 ± 0.6 mm ZOI observed for the CA-EA extract at 1000 µg/mL and 2000 µg/mL, respectively. A similar trend was observed against *S. epidermidis* (G+), where the AgNPs showed a ZOI of 13.67 ± 0.6 mm, compared to 9.33 ± 0.6 mm and 9.67 ± 0.6 mm for the extract concentrations. For the Gram-negative bacteria, CA-EA-AgNPs produced a ZOI of 15.67 ± 0.6 mm against *P. aeruginosa*, surpassing the 9.67 ± 0.6 mm and 10.67 ± 0.6 mm shown by the extract. Most significantly, against *P. mirabilis* (G−), the CA-EA-AgNPs demonstrated a ZOI of 17.67 ± 0.6 mm, markedly higher than the 10.00 ± 1.00 mm

Bacterial Strain	CA-EA- extract (1000 µg/mL)	CA-EA- extract (2000 µg/mL)	CA-EA-AgNPs (10 mM)	Streptomycin (standard)
(a) *S. aureus*				
(b) *S. epidermidis*				
(c) *P. aeruginosa*				
(d) *P. mirabilis*				

Fig. 9 Antibacterial activity of CA-EA extracts, CA-EA-AgNPs, and streptomycin (standard) against (a) *S. aureus*, (b) *S. epidermidis*, (c) *P. aeruginosa*, and (d) *P. mirabilis*

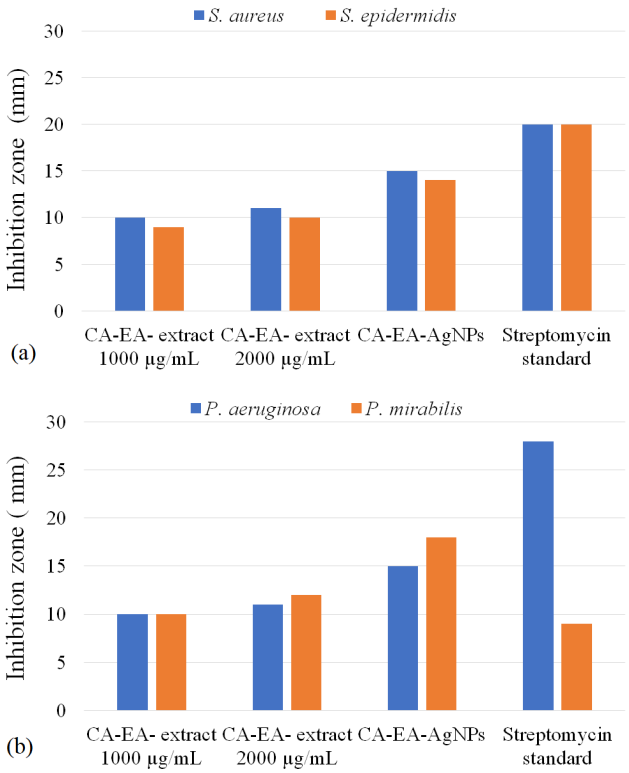

Fig. 10 Antibacterial activity against (a) Gram-positive bacteria, (b) Gram-negative bacteria

and 11.67 ± 0.6 mm recorded for the CA-EA extract. While the standard antibiotic streptomycin showed higher activity against *S. aureus* (20.33 ± 0.6 mm), *S. epidermidis* (19.67 ± 0.6 mm), and *P. aeruginosa* (27.67 ± 0.6 mm), it was less effective against *P. mirabilis* (8.33 ± 0.6 mm) compared to the CA-EA-AgNPs (17.67 ± 0.6 mm). These results clearly indicate that the incorporation of silver nanoparticles significantly enhances the antibacterial potency of the CA-EA extract against all tested bacterial strains.

The enhanced activity of AgNPs is attributed to their nanoscale size, large surface area, and ability to release Ag^+ ions, which can disrupt cell membranes, interfere with respiratory enzymes, and damage DNA [18, 19]. AgNPs primarily disrupt microbial membranes by adhering to

Table 4 Antibacterial activity (zone of inhibition in mm) of CA-EA extract and CA-EA-AgNPs

Test sample	Zone of inhibition in mm against bacteria			
	S. aureus G+	*S. epidermidis* G+	*P. aeruginosa* G−	*P. mirabilis* G−
CA-EA- extract (<1000 µg/mL)	NZ	NZ	NZ	NZ
CA-EA- extract (1000 µg/mL)	9.67 ± 0.6	9.33 ± 0.6	9.67 ± 0.6	10.00 ± 1.00
CA-EA- extract (2000 µg/mL)	10.67 ± 0.6	9.67 ± 0.6	10.67 ± 0.6	11.67 ± 0.6
CA-EA-AgNPs (10 mM)	15.00 ± 1.00	13.67 ± 0.6	15.67 ± 0.6	17.67 ± 0.6
Streptomycin (standard)	20.33 ± 0.6	19.67 ± 0.6	27.67 ± 0.6	8.33 ± 0.6

*NZ: No Zone; G+: Gram-positive; G−: Gram-negative

the cell wall, causing structural damage, increasing permeability, and inducing pit formation. These mechanisms lead to electrolyte leakage, loss of membrane potential, and ultimately cell death, often enhanced by the release of Ag^+ ions from the nanoparticles [83–85]. Many phytochemicals are themselves intrinsically antimicrobial. These phytochemicals on the surface of nanoparticles form a bioorganic corona and make them more stable against aggregation, and improve surface area, which in turn improves their bioactivity. This organic capping layer controls the release of Ag^+ ions, provides sustained antimicrobial action, and prolongs and controls toxicity toward microbes. Plant-mediated AgNPs enhance drug uptake and therapeutic efficiency through a mechanism combining biocompatible stabilization, size-dependent cell penetration, and synergistic membrane disruption. These nanoparticles act as efficient carriers, often improving the delivery of drugs to target cells while reducing toxicity compared to chemically synthesized alternatives. Plant-mediated AgNPs, which are often coated with phytochemicals like polyphenols or flavonoids, show enhanced biological activity [86]. Due to the affinity of silver ions to sulfur-containing proteins and their binding to respiratory enzymes, they inhibit electron transfer, and that stops ATP production, and cells lose their energy. Ag^+ ions interact with the sulfur and phosphorus components of DNA, causing it to condense and prevent replication and cell [87–89].

Gram-negative bacteria, with their thinner peptidoglycan layer, are sometimes reported to be more susceptible to AgNPs, though this can vary [89] [66]. In the present study also, *P. mirabilis*, a Gram-negative bacterium, showed slightly higher susceptibility. Gram-negative bacteria have a single layer of peptidoglycan in their cell membrane, whereas Gram-positive bacteria have multiple layers of peptidoglycan in their membrane, which makes them more rigid. This slight difference may be caused by the different composition of their cell walls [90]. The negative charge of the bacterial cell wall draws the silver ions from the nanoparticles, and when they encounter an electrostatic attraction, they move and adhere to the wall, changing its permeability and ultimately changing the composition of the cell wall [91].

3.5 Antifungal and synergistic activity against *Malassezia furfur*

The antifungal activity of CA-EA-AgNPs alone and in combination with ketoconazole (a standard antifungal drug) was tested against the dandruff-causing yeast *M. furfur*. The inhibition zones are summarized in Table 5. Fig. 11(a) shows the agar well diffusion inhibition zones, which are presented graphically in Fig. 11(b).

The antidandruff potential of the synthesized CA-EA-AgNPs, both alone and in combination with a standard antifungal, was evaluated against *M. furfur*, with demineralized (DM) water serving as a negative control. As expected, DM water exhibited no zone of inhibition (NZ) in either the single plate or comparative assays. The CA-EA-AgNPs (5 mM) demonstrated moderate antifungal activity, producing a zone of inhibition of 11 ± 0.5 mm in both assay conditions. Ketoconazole (0.5 mg/mL), a known antifungal agent, showed a more pronounced effect, with zones of inhibition of 15 ± 0.9 mm (single plate) and 16 ± 0.9 mm (comparative).

Table 5 Antifungal activity (zone of inhibition in mm) against *Malassezia furfur*

Test sample and concentration	Zone of inhibition (mm)	
	Single plate	Comparative
DM water	NZ	NZ
CA-EA-AgNPs (5 mM)	11 ± 0.5	11 ± 0.5
Ketoconazole (0.5 mg/mL)	15 ± 0.9	16 ± 0.9
Ketoconazole (0.5 mg/mL) + CA-EA-AgNPs (5 mM)	18 ± 0.8	19 ± 0.8

*NZ: No zone

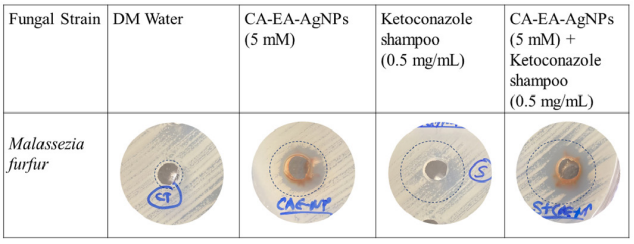

(a)

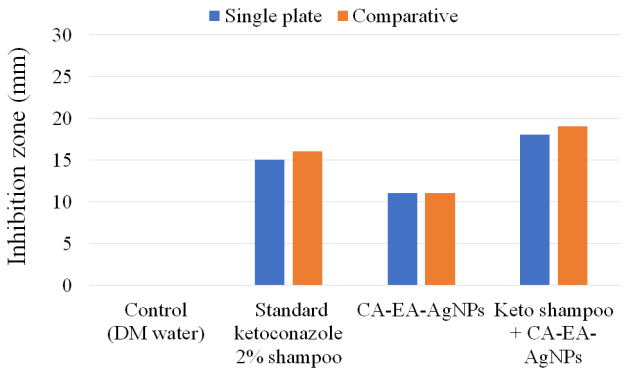

(b)

Fig. 11 (a) Antifungal activity against *Malassezia furfur*. (Wells: 1-DM water, 2-CA-EA-AgNPs (5mM), 3-ketoconazole (500 µg/mL), 4-CA-EA-AgNPs (5 mM) + ketoconazole (500 µg/mL), (b) antibacterial activity against dandruff-causing fungus *M. furfur*.

Notably, when CA-EA-AgNPs (5 mM) were combined with ketoconazole (0.5 mg/mL), the resulting zone of inhibition was further enhanced to 18 ± 0.7 mm (single plate) and 19 ± 0.7 mm (comparative). This increased inhibitory effect of the combination surpasses the activity of either ketoconazole or CA-EA-AgNPs, when used individually, indicates a synergistic interaction between the nanoparticles and the conventional antifungal drug against *M. furfur*. This synergy could be due to AgNPs disrupting the fungal cell wall/membrane, thereby facilitating increased uptake or efficacy of ketoconazole, which inhibits ergosterol synthesis [72, 90]. Silver nanoparticles (AgNPs) and ketoconazole work together to combat *Malassezia furfur* through a dual-action mechanism that targets both the cell's internal metabolic processes and its external defenses. Silver nanoparticles can have fungicidal activity (kill the fungus), which results in total eradication when combined with ketoconazole, which is largely fungistatic (inhibits growth) [92]. The silver nanoparticles induced inside the cell produce reactive oxygen species that create more oxidative stress to the cell and damage the mitochondrial membrane and structure of fungi [93]. The phytochemicals present in the extract have beneficial antioxidant properties (reducing power capacity), and the antimicrobial capacity itself is acting synergistically with silver nanoparticles to enhance antimicrobial and antifungal activity [29]. Mussin and Giusiano reported the mechanisms of action of AgNPs and ketoconazole on fungi, but the combination of both is efficacious due to their synergistic effect [92]. This is the first report of AgNPs from *C. anthelminticum* exhibiting activity against *M. furfur* and synergism with ketoconazole.

4 Conclusion

This study successfully demonstrated a simple, eco-friendly, and cost-effective method for the biogenic synthesis of silver nanoparticles using an ethyl acetate extract of *Centratherum anthelminticum* seeds. The synthesized CA-EA-AgNPs were spherical and crystalline, with an average size of ~46 nm (DLS), ~16-27 nm (FESEM), and ~11-17 nm (TEM), and exhibited moderate stability. Phytochemicals present in the seed extract, particularly polyphenols and flavonoids, acted as effective reducing and capping agents. The CA-EA-AgNPs displayed significantly enhanced broad-spectrum antibacterial activity against both Gram-positive and Gram-negative bacteria compared to the crude extract. Crucially, this research is the first to report the antifungal activity of *C. anthelminticum* seed extract-derived AgNPs against *Malassezia furfur*, the causative agent of dandruff. Furthermore, a notable synergistic effect was observed when CA-EA-AgNPs were combined with ketoconazole, suggesting their potential to improve the efficacy of conventional antifungal treatments and possibly combat drug resistance. These findings underscore the potential of *C. anthelminticum* as a valuable natural resource for green nanotechnology and highlight the promise of CA-EA-AgNPs for various biomedical applications, especially in developing novel antimicrobial and antifungal formulations for skin and soft tissue infections. Future studies should focus on elucidating the precise mechanisms of synergy and evaluating the in vivo efficacy and safety of these nanoparticles.

References

[1] Mohammad, Z. H., Ahmad, F., Ibrahim, S. A., Zaidi, S. "Application of nanotechnology in different aspects of the food industry", Discover Food, 2(1), 12, 2022. https://doi.org/10.1007/s44187-022-00013-9

[2] Bayda, S., Adeel, M., Tuccinardi, T., Cordani, M., Rizzolio, F. "The History of Nanoscience and Nanotechnology: From Chemical–Physical Applications to Nanomedicine", Molecules, 25(1), 112, 2020. https://doi.org/10.3390/molecules25010112

[3] Joudeh, N., Linke, D. "Nanoparticle classification, physicochemical properties, characterization, and applications: a comprehensive review for biologists", Journal of Nanobiotechnology, 20(1), 262, 2022. https://doi.org/10.1186/s12951-022-01477-8

[4] Roduner, E. "Size matters: Why nanomaterials are different", Chemical Society Reviews, 35(7), pp. 583–592, 2006. https://doi.org/10.1039/b502142c

[5] Zhang, X.-F., Liu, Z.-G., Shen, W., Gurunathan, S. "Silver Nanoparticles: Synthesis, Characterization, Properties, Applications, and Therapeutic Approaches", International Journal of Molecular Sciences, 17(9), 1534, 2016. https://doi.org/10.3390/ijms17091534

[6] Azharuddin, M., Zhu, G. H., Das, D., Ozgur, E., Uzun, L., Turner, A. P. F., Patra, H. K. "A repertoire of biomedical applications of noble metal nanoparticles", Chemical Communications, 55(49), pp. 6964–6996, 2019. https://doi.org/10.1039/c9cc01741k

[7] Gavade, N. L., Kadam, A. N., Suwarnkar, M. B., Ghodake, V. P., Garadkar, K. M. "Biogenic synthesis of multi-applicative silver nanoparticles by using Ziziphus Jujuba leaf extract", Spectrochimica Acta - Part A: Molecular and Biomolecular Spectroscopy, 136, pp. 953–960, 2015. https://doi.org/10.1016/j.saa.2014.09.118

[8] Kgatshe, M., Aremu, O. S., Katata-Seru, L., Gopane, R. "Characterization and Antibacterial Activity of Biosynthesized Silver Nanoparticles Using the Ethanolic Extract of Pelargonium sidoides DC", Journal of Nanomaterials, 2019(1), 3501234, 2019. https://doi.org/10.1155/2019/3501234

[9] Ahmed, S., Ahmad, M., Swami, B. L., Ikram, S. "A review on plants extract mediated synthesis of silver nanoparticles for antimicrobial applications: A green expertise", Journal of Advanced Research, 7(1), pp. 17–28, 2016. https://doi.org/10.1016/j.jare.2015.02.007

[10] Egbuna, C., Parmar, V. K., Jeevanandam, J., Ezzat, S. M., Patrick-Iwuanyanwu, K. C., Adetunji, C. O., … Ibeabuchi, C. G. "Toxicity of Nanoparticles in Biomedical Application: Nanotoxicology", Journal of Toxicology, 2021(1), 954443, 2021. https://doi.org/10.1155/2021/9954443

[11] Mittal, A. K., Chisti, Y., Banerjee, U. C. "Synthesis of metallic nanoparticles using plant extracts", Biotechnology Advances, 31(2), pp. 346–356, 2013. https://doi.org/10.1016/j.biotechadv.2013.01.003

[12] Bao, Y., He, J., Song, K., Guo, J., Zhou, X., Liu, S. "Plant-Extract-Mediated Synthesis of Metal Nanoparticles", Journal of Chemistry, 2021(1), 6562687, 2021. https://doi.org/10.1155/2021/6562687

[13] Magdum, A. B., Waghmode, R. S., Shinde, K. V., Mane, M. P., Kamble, M. V., Kamble, R. S., … Nimbalkar, M. S. "Biogenic synthesis of silver nanoparticles from leaves extract of *Decaschistia trilobata* an endemic shrub and its application as antioxidant, antibacterial, anti-inflammatory and dye reduction", Catalysis Communications, 187, 106865, 2024. https://doi.org/10.1016/j.catcom.2024.106865

[14] Panja, A., Mishra, A. K., Dash, M., Singh, S. K., Kumar, B., Pandey, N. K. "Silver Nanoparticles – A Review", 5(2), pp. 95–102, 2021. https://doi.org/10.14744/ejmo.2021.59602

[15] Siddiqi, K. S., Husen, A., Rao, R. A. K. "A review on biosynthesis of silver nanoparticles and their biocidal properties", Journal of Nanobiotechnology, 16(1), 14, 2018. https://doi.org/10.1186/s12951-018-0334-5

[16] Mukaratirwa-Muchanyereyi, N., Gusha, C., Mujuru, M., Guyo, U., Nyoni, S. "Synthesis of silver nanoparticles using plant extracts from *Erythrina abyssinica* aerial parts and assessment of their anti-bacterial and anti-oxidant activities", Results in Chemistry, 4, 100402, 2022. https://doi.org/10.1016/j.rechem.2022.100402

[17] Mikhailova, E. O. "Silver Nanoparticles: Mechanism of Action and Probable Bio-Application", Journal of Functional Biomaterials, 11(4), 84, 2020. https://doi.org/10.3390/jfb11040084

[18] Slavin, Y. N., Asnis, J., Häfeli, U. O., Bach, H. "Metal nanoparticles: Understanding the mechanisms behind antibacterial activity", Journal of Nanobiotechnology, 15(1), 65, 2017. https://doi.org/10.1186/s12951-017-0308-z

[19] Durán, N., Durán, M., de Jesus, M. B., Seabra, A. B., Fávaro, W. J., Nakazato, G. "Silver nanoparticles: A new view on mechanistic aspects on antimicrobial activity", Nanomedicine: Nanotechnology, Biology and Medicine, 12(3), pp. 789–799, 2016. https://doi.org/10.1016/j.nano.2015.11.016

[20] Herdiana, Y. "Nanoparticles of natural product-derived medicines: Beyond the pandemic", Heliyon, 11(4), e42739, 2025. https://doi.org/10.1016/j.heliyon.2025.e42739

[21] Khoobchandani, M., Katti, K. K., Karikachery, A. R., Thipe, V. C., Srisrimal, D., Mohandoss, D. K. D., … Katti, K. V. "New approaches in breast cancer therapy through green nanotechnology and nano-ayurvedic medicine – pre-clinical and pilot human clinical investigations", International Journal of Nanomedicine, 15, pp. 181–197, 2020. https://doi.org/10.2147/IJN.S219042

[22] Dogra, N. K., Kumar, S., Kumar, D. "Vernonia anthelmintica (L.) Willd.: An ethnomedicinal, phytochemical, pharmacological and toxicological review", Journal of Ethnopharmacology, 256, 112777, 2020. https://doi.org/10.1016/j.jep.2020.112777

[23] Mehta, B. K., Mehta, D., Verma, M. "Novel steroids from the seeds of Centratherum anthelminticum", Natural Product Research, 19(5), pp. 435–442, 2005. https://doi.org/10.1080/14786410512331330729

[24] Rolnik, A., Olas, B. "The Plants of the Asteraceae Family as Agents in the Protection of Human Health", International Journal of Molecular Sciences, 22(6), 3009, 2021. https://doi.org/10.3390/ijms22063009

[25] Vanlalveni, C., Lallianrawna, S., Biswas, A., Selvaraj, M., Changmai, B., Rokhum, S. L. "Green synthesis of silver nanoparticles using plant extracts and their antimicrobial activities: a review of recent literature", RSC Advances, 11(5), pp. 2804–2837, 2021. https://doi.org/10.1039/D0RA09941D

[26] De Mel, S., Gruenler, J., Khoury, L., Heynes, A., Frazekas, J., Damaske, K., … Anderson, R. S. "Green Synthesized *Magnolia alba* Silver Nanoparticles Kill Pathogens, Inhibit Cancer, and Display Antioxidant and Photocatalytic Properties", 2024, December 28. https://doi.org/10.1101/2024.12.27.630567

[27] Maki, M. A. A., Tan, K. F., Yee, M. T. S., Mishra, D. K., Venkatesh, M. P., Abduljaleel, O. W., … Palanirajan, V. K. "Green solvents as a sustainable strategy to reduce the impact of hazardous waste on human health", Discover Chemistry, 2(1), 342, 2025. https://doi.org/10.1007/s44371-025-00450-2

[28] Shahzadi, S., Fatima, S., Ul Ain, Q., Shafiq, Z., Janjua, M. R. S. A. "A review on green synthesis of silver nanoparticles (SNPs) using plant extracts: A multifaceted approach in photocatalysis, environmental remediation, and biomedicine", RSC Advances, 15(5), pp. 3858–3903, 2025. https://doi.org/10.1039/d4ra07519f

[29] Eker, F., Akdaşçi, E., Duman, H., Bechelany, M., Karav, S. "Green Synthesis of Silver Nanoparticles Using Plant Extracts: A Comprehensive Review of Physicochemical Properties and Multifunctional Applications", International Journal of Molecular Sciences, 26(13), 6222, 2025. https://doi.org/10.3390/ijms26136222

[30] Khan, A., Younis, T., Anas, M., Ali, M., Shinwari, Z. K., Khalil, A. T., … Khan, N. "Withania coagulans-mediated green synthesis of silver nanoparticles: characterization and assessment of their phytochemical, antioxidant, toxicity, and antimicrobial activities", BMC Plant Biology, 25(1), 574, 2025. https://doi.org/10.1186/s12870-025-06533-7

[31] Akhtar, W., Hamza, M. I., Qayyum, S., Khan, M. A., Mukhtar, N., Kamal, A., … Naseem, M. T. "Phyto-synthesis, characterization of silver nanoparticles from mint leaf extract and its evaluation in antimicrobial and pharmacological applications", BMC Plant Biology, 25(1), 1072, 2025.
https://doi.org/10.1186/s12870-025-07043-2

[32] U Din, M. M., Batool, A., Ashraf, R. S., Yaqub, A., Rashid, A., U Din, N. M. "Green Synthesis and Characterization of Biologically Synthesized and Antibiotic-Conjugated Silver Nanoparticles followed by Post-Synthesis Assessment for Antibacterial and Antioxidant Applications", ACS Omega, 9(17), pp. 18909–18921, 2024.
https://doi.org/10.1021/acsomega.3c08927

[33] Binsalah, M., Devanesan, S., AlSalhi, M. S., Nooh, A., Alghamdi, O., Nooh, N. "Biomimetic Synthesis of Silver Nanoparticles Using Ethyl Acetate Extract of Urtica diocia Leaves; Characterizations and Emerging Antimicrobial Activity", Microorganisms, 10(4), 789, 2022.
https://doi.org/10.3390/microorganisms10040789

[34] Jaison, J. P., Balasubramanian, B., Gangwar, J., James, N., Pappuswamy, M., Anand, A. V., … Sebastian, J. K. "Green Synthesis of Bioinspired Nanoparticles Mediated from Plant Extracts of *Asteraceae* Family for Potential Biological Applications", Antibiotics, 12(3), 543, 2023.
https://doi.org/10.3390/antibiotics12030543

[35] Geremu, M., Tola, Y. B., Sualeh, A. "Extraction and determination of total polyphenols and antioxidant capacity of red coffee (*Coffea arabica* L.) pulp of wet processing plants", Chemical and Biological Technologies in Agriculture, 3(1), 25, 2016.
https://doi.org/10.1186/s40538-016-0077-1

[36] Formagio, A. S. N., Volobuff, C. R. F., Santiago, M., Cardoso, C. A. L., Vieira, M. D. C., Pereira, Z. V. "Evaluation of antioxidant activity, total flavonoids, tannins and phenolic compounds in *Psychotria* leaf extracts", Antioxidants, 3(4), pp. 745–757, 2014.
https://doi.org/10.3390/antiox3040745

[37] Bhalodia, N., Nariya, P., Acharya, R., Shukla, V. "*In vitro* antioxidant activity of hydro alcoholic extract from the fruit pulp of *Cassia fistula* Linn.", AYU (An international quarterly journal of research in Ayurveda), 34(2), pp. 209–213, 2013.
https://doi.org/10.4103/0974-8520.119684

[38] Kumar, V., Yadav, S. C., Yadav, S. K. "*Syzygium cumini* leaf and seed extract mediated biosynthesis of silver nanoparticles and their characterization", Journal of Chemical Technology and Biotechnology, 85(10), pp. 1301–1309, 2010.
https://doi.org/10.1002/jctb.2427

[39] Liu, H., Zhang, H., Wang, J., Wei, J. "Effect of temperature on the size of biosynthesized silver nanoparticle: Deep insight into microscopic kinetics analysis", Arabian Journal of Chemistry, 13(1), pp. 1011–1019, 2020.
https://doi.org/10.1016/j.arabjc.2017.09.004

[40] Htwe, Y. Z. N., Chow, W. S., Suda, Y., Mariatti, M. "Effect of silver nitrate concentration on the production of silver nanoparticles by green method", Materials Today: Proceedings, 17, pp. 568–573, 2019.
https://doi.org/10.1016/j.matpr.2019.06.336

[41] Veerasamy, R., Xin, T. Z., Gunasagaran, S., Xiang, T. F. W., Yang, E. F. C., Jeyakumar, N., Dhanaraj, S. A. "Biosynthesis of silver nanoparticles using mangosteen leaf extract and evaluation of their antimicrobial activities", Journal of Saudi Chemical Society, 15(2), pp. 113–120, 2011.
https://doi.org/10.1016/j.jscs.2010.06.004

[42] Izak-Nau, E., Huk, A., Reidy, B., Uggerud, H., Vadset, M., Eiden, S., … Lynch, I. "Impact of storage conditions and storage time on silver nanoparticles' physicochemical properties and implications for their biological effects", RSC Advances, 5(102), pp. 84172–84185, 2015.
https://doi.org/10.1039/c5ra10187e

[43] Anith Jose, R., Devina Merin, D., Arulananth, T. S., Shaik, N. "Characterization Analysis of Silver Nanoparticles Synthesized from *Chaetoceros calcitrans*", Journal of Nanomaterials, 2022(1), 056551,, 2022.
https://doi.org/10.1155/2022/4056551

[44] Jyoti, K., Baunthiyal, M., Singh, A. "Characterization of silver nanoparticles synthesized using *Urtica dioica* Linn. leaves and their synergistic effects with antibiotics", Journal of Radiation Research and Applied Sciences, 9(3), pp. 217–227, 2016.
https://doi.org/10.1016/j.jrras.2015.10.002

[45] Alam, M. "Analyses of biosynthesized silver nanoparticles produced from strawberry fruit pomace extracts in terms of biocompatibility, cytotoxicity, antioxidant ability, photodegradation, and in-silico studies", Journal of King Saud University - Science, 34(8), 102327, 2022.
https://doi.org/10.1016/j.jksus.2022.102327

[46] Goudarzi, M., Mir, N., Mousavi-Kamazani, M., Bagheri, S., Salavati-Niasari, M. "Biosynthesis and characterization of silver nanoparticles prepared from two novel natural precursors by facile thermal decomposition methods", Scientific Reports, 6, 32539, 2016.
https://doi.org/10.1038/srep32539

[47] Vanaja, M., Rajeshkumar, S., Paulkumar, K., Gnanajobitha, G., Malarkodi, C., Annadurai, G. "Phytosynthesis and characterization of silver nanoparticles using stem extract of *Coleus aromaticus*", International Journal of Materials and Biomaterials Applications, 3(1), 17, 2013.

[48] Sunkar, S., Nachiyar, C. V. "Biogenesis of antibacterial silver nanoparticles using the endophytic bacterium *Bacillus cereus* isolated from *Garcinia xanthochymus*", Asian Pacific Journal of Tropical Biomedicine, 2(12), pp. 953–959, 2012.
https://doi.org/10.1016/S2221-1691(13)60006-4

[49] Balouiri, M., Sadiki, M., Ibnsouda, S. K. "Methods for *in vitro* evaluating antimicrobial activity: A review", Journal of Pharmaceutical Analysis, 6(2), pp. 71–79, 2016.
https://doi.org/10.1016/j.jpha.2015.11.005

[50] Kahsay, M. H., RamaDevi, D., Kumar, Y. P., Mohan, B. S., Tadesse, A., Battu, G., Basavaiah, K. "Synthesis of silver nanoparticles using aqueous extract of *Dolichos lablab* for reduction of 4-Nitrophenol, antimicrobial and anticancer activities", OpenNano, 3, pp. 28–37, 2018.
https://doi.org/10.1016/j.onano.2018.04.001

[51] Azhdarzadeh, M., Lotfipour, F., Zakeri-Milani, P., Mohammadi, G., Valizadeh, H. "Anti-bacterial performance of azithromycin nanoparticles as colloidal drug delivery system against different gram-negative and gram-positive bacteria", Advanced Pharmaceutical Bulletin, 2(1), pp. 17–24, 2012. https://doi.org/10.5681/apb.2012.003

[52] Laokor, N., Juntachai, W. "Exploring the antifungal activity and mechanism of action of Zingiberaceae rhizome extracts against *Malassezia furfur*", Journal of Ethnopharmacology, 279, 114354, 2021. https://doi.org/10.1016/j.jep.2021.114354

[53] Moond, M., Singh, S., Sangwan, S., Rani, S., Beniwal, A., Rani, J., … Devi, P. "Phytofabrication of Silver Nanoparticles Using *Trigonella foenum-graceum* L. Leaf and Evaluation of Its Antimicrobial and Antioxidant Activities", International Journal of Molecular Sciences, 24(4), 3480, 2023. https://doi.org/10.3390/ijms24043480

[54] Khan, M., Khan, T., Wahab, S., Aasim, M., Sherazi, T. A., Zahoor, M., Yun, S.-I. "Solvent based fractional biosynthesis, phytochemical analysis, and biological activity of silver nanoparticles obtained from the extract of *Salvia moorcroftiana*", PLOS ONE, 18(10), e0287080, 2023. https://doi.org/10.1371/journal.pone.0287080

[55] Ashraf, J. M., Ansari, M. A., Khan, H. M., Alzohairy, M. A., Choi, I. "Green synthesis of silver nanoparticles and characterization of their inhibitory effects on AGEs formation using biophysical techniques", Scientific Reports, 6(1), 20414, 2016. https://doi.org/10.1038/srep20414

[56] Jain, P. K., Qian, W., El-Sayed, M. A. "Ultrafast electron relaxation dynamics in coupled metal nanoparticles in aggregates", Journal of Physical Chemistry B, 110(1), pp. 136–142, 2006. https://doi.org/10.1021/jp055562p

[57] Sharma, V. K., Yngard, R. A., Lin, Y. "Silver nanoparticles: Green synthesis and their antimicrobial activities", Advances in Colloid and Interface Science, 145(1–2), pp. 83–96, 2009. https://doi.org/10.1016/j.cis.2008.09.002

[58] Handayani, W., Ningrum, A. S., Imawan, C. "The Role of pH in Synthesis Silver Nanoparticles Using *Pometia pinnata* (Matoa) Leaves Extract as Bioreductor", Journal of Physics: Conference Series, 1428(1), 012021, 2020. https://doi.org/10.1088/1742-6596/1428/1/012021

[59] Liaqat, N., Jahan, N., Khalil-ur-Rahman, Anwar, T., Qureshi, H. "Green synthesized silver nanoparticles: Optimization, characterization, antimicrobial activity, and cytotoxicity study by hemolysis assay", Frontiers in Chemistry, 10, 952006, 2022. https://doi.org/10.3389/fchem.2022.952006

[60] Borowik, A., Butowska, K., Konkel, K., Banasiuk, R., Derewonko, N., Wyrzykowski, D., … Piosik, J. "The impact of surface functionalization on the biophysical properties of silver nanoparticles", Nanomaterials, 9(7), 973, 2019. https://doi.org/10.3390/nano9070973

[61] Mondéjar-López, M., López-Jiménez, A. J., Abad-Jordá, M., Rubio-Moraga, A., Ahrazem, O., Gómez-Gómez, L., Niza, E. "Biogenic silver nanoparticles from iris tuberosa as potential preservative in cosmetic products", Molecules, 26(15), 4696, 2021. https://doi.org/10.3390/molecules26154696

[62] Raja, S., Ramesh, V., Thivaharan, V. "Green biosynthesis of silver nanoparticles using *Calliandra haematocephala* leaf extract, their antibacterial activity and hydrogen peroxide sensing capability", Arabian Journal of Chemistry, 10(2), pp. 253–261, 2017. https://doi.org/10.1016/j.arabjc.2015.06.023

[63] Anil Kumar, H. S., Bhavi, S. M., Singh, S. R., Thokchom, B., Yarajarla, R. B., Kotresha, D. "Biosynthesis of silver nanoparticles using *Aristolochia bracteolata* Lam. ethyl acetate extract: Characterization and *In Vitro* anticancer activity against lung adenocarcinoma cells", Next Nanotechnology, 7, 100174, 2025. https://doi.org/10.1016/j.nxnano.2025.100174

[64] Khakhalary, S., Narzari, S. "Phytochemical profiling and FTIR analysis of aqueous extracts from three selected ethnomedicinal plants of North East India", Current Botany, 16, pp. 45–52, 2025. https://doi.org/10.25081/cb.2025.v16.9117

[65] Sancheti, R. S., Samreen, S., Gite, A. B., Patil, P. N., Patil, M. P., Shah, H. H., … Patil, M. T. "*Cordia sebestena* leaf extract mediated biosynthesis of silver nanoparticles, characterization, and screening of its antimicrobial activities", Green Analytical Chemistry, 6, 100075, 2023. https://doi.org/10.1016/j.greeac.2023.100075

[66] Ryntathiang, I., Behera, A., Richard, T., Dharmalingam Jothinathan, M. K. "An Assessment of the *In Vitro* Antioxidant Activity of Cobalt Nanoparticles Synthesized From *Millettia pinnata*, *Butea monosperma*, and *Madhuca indica* Extracts: A Comparative Study", Cureus, 16(4), e59112, 2024. https://doi.org/10.7759/cureus.59112

[67] Md Salim, R., Asik, J., Sarjadi, M. S. "Chemical functional groups of extractives, cellulose and lignin extracted from native *Leucaena leucocephala* bark", Wood Science and Technology, 55(2), pp. 295–313, 2021. https://doi.org/10.1007/s00226-020-01258-2

[68] Raj, T. L. S., Vijayakumari, J., Kavitha, S. "Green Synthesis of Silver Nanoparticles Using *Murraya koenigii* Leaf Extract and Their Antibacterial Potential", 8(3), pp. 76–81, 2018. https://doi.org/10.37591/rrjols.v8i3.1219

[69] Jemal, K., Sandeep, B. V., Pola, S. "Synthesis, Characterization, and Evaluation of the Antibacterial Activity of *Allophylus serratus* Leaf and Leaf Derived Callus Extracts Mediated Silver Nanoparticles", Journal of Nanomaterials, 2017, 4213275, 2017. https://doi.org/10.1155/2017/4213275

[70] Elbasuney, S., Attwa, M., Deif, A., ElGamal, M., Fayoud, A., Abdelkhalek, S. M., Gobara, M. "Green synthesis and catalytic activity assessment of bespoke nano-catalyst for eco-friendly green propellant systems based on hydrogen peroxide", Brazilian Journal of Chemical Engineering, 41(4), pp. 1151–1164, 2024. https://doi.org/10.1007/s43153-023-00380-5

[71] Hijazi, B. U., Faraj, M., Mhanna, R., El-Dakdouki, M. H. "Biosynthesis of silver nanoparticles as a reliable alternative for the catalytic degradation of organic dyes and antibacterial applications", Current Research in Green and Sustainable Chemistry, 8, 100408, 2024. https://doi.org/10.1016/j.crgsc.2024.100408

[72] Dhaka, A., Chand Mali, S., Sharma, S., Trivedi, R. "A review on biological synthesis of silver nanoparticles and their potential applications", Results in Chemistry, 6, 101108, 2023. https://doi.org/10.1016/j.rechem.2023.101108

[73] Velgosova, O., Dolinská, S., Podolská, H., Mačák, L., Čižmárová, E. "Impact of Plant Extract Phytochemicals on the Synthesis of Silver Nanoparticles", Materials, 17(10), 2252, 2024. https://doi.org/10.3390/ma17102252

[74] Kuppusamy, P., Yusoff, M. M., Maniam, G. P., Govindan, N. "Biosynthesis of metallic nanoparticles using plant derivatives and their new avenues in pharmacological applications – An updated report", Saudi Pharmaceutical Journal, 24(4), pp. 473–484, 2016. https://doi.org/10.1016/j.jsps.2014.11.013

[75] Mustapha, T., Misni, N., Ithnin, N. R., Daskum, A. M., Unyah, N. Z. "A Review on Plants and Microorganisms Mediated Synthesis of Silver Nanoparticles, Role of Plants Metabolites and Applications", International Journal of Environmental Research and Public Health, 19(2), 674, 2022. https://doi.org/10.3390/ijerph19020674

[76] Alzubaidi, A. K., Al-Kaabi, W. J., Ali, A. Al, Albukhaty, S., Al-Karagoly, H., Sulaiman, G. M., … Khane, Y. "Green Synthesis and Characterization of Silver Nanoparticles Using Flaxseed Extract and Evaluation of Their Antibacterial and Antioxidant Activities", Applied Sciences, 13(4), 2182, 2023. https://doi.org/10.3390/app13042182

[77] Helmlinger, J., Sengstock, C., Groß-Heitfeld, C., Mayer, C., Schildhauer, T. A., Köller, M., Epple, M. "Silver nanoparticles with different size and shape: Equal cytotoxicity, but different antibacterial effects", RSC Advances, 6(22), pp. 18490–18501, 2016. https://doi.org/10.1039/c5ra27836h

[78] Sabapathi, N., Ramalingam, S., Aruljothi, K. N., Lee, J., and Barathi, S. "Characterization and Therapeutic Applications of Biosynthesized Silver Nanoparticles Using *Cassia auriculate* Flower Extract", Plants, 12(4), 707, 2023. https://doi.org/10.3390/plants12040707

[79] Singh, H., Du, J., Yi, T. H. "*Kinneretia* THG-SQI4 mediated biosynthesis of silver nanoparticles and its antimicrobial efficacy", Artificial Cells, Nanomedicine and Biotechnology, 45(3), pp. 602–608, 2017. https://doi.org/10.3109/21691401.2016.1163718

[80] Karunakaran, G., Sudha, K. G., Ali, S., Cho, E.-B. "Biosynthesis of Nanoparticles from Various Biological Sources and Its Biomedical Applications", Molecules, 28(11), 4527, 2023. https://doi.org/10.3390/molecules28114527

[81] Hussein, H. S., Ngugi, C., Tolo, F. M., Maina, E. N. "Anticancer potential of silver nanoparticles biosynthesized using *Catharanthus roseus* leaves extract on cervical (HeLa229) cancer cell line", Scientific African, 25, e02268, 2024. https://doi.org/10.1016/j.sciaf.2024.e02268

[82] Khan, I., Saeed, K., Khan, I. "Nanoparticles: Properties, applications and toxicities", Arabian Journal of Chemistry, 12(7), pp. 908–931, 2019. https://doi.org/10.1016/j.arabjc.2017.05.011

[83] More, P. R., Pandit, S., Filippis, A. De, Franci, G., Mijakovic, I., Galdiero, M. "Silver Nanoparticles: Bactericidal and Mechanistic Approach against Drug Resistant Pathogens", Microorganisms, 11(2), 369, 2023. https://doi.org/10.3390/microorganisms11020369

[84] Simon, S., Sibuyi, N. R. S., Fadaka, A. O., Meyer, S., Josephs, J., Onani, M. O., … Madiehe, A. M. "Biomedical Applications of Plant Extract-Synthesized Silver Nanoparticles", Biomedicines, 10(11), 2792, 2022. https://doi.org/10.3390/biomedicines10112792

[85] Sheydaei, M., Edraki, M., Radeghi Mehrjou, S. M. "Anticorrosion and Antimicrobial Evaluation of Sol-Gel Hybrid Coatings Containing *Clitoria ternatea* Modified Clay", Gels, 9(6), 490, 2023. https://doi.org/10.3390/gels9060490

[86] Dhir, R., Chauhan, S., Subham, P., Kumar, S., Sharma, P., Shidiki, A., Kumar, G. "Plant-mediated synthesis of silver nanoparticles: unlocking their pharmacological potential–a comprehensive review", Frontiers in Bioengineering and Biotechnology, 11, 1324805, 2024. https://doi.org/10.3389/fbioe.2023.1324805

[87] Abdel-Hadi, A., Iqbal, D., Alharbi, R., Jahan, S., Darwish, O., Alshehri, B., … Fatima, F. "Myco-Synthesis of Silver Nanoparticles and Their Bioactive Role against Pathogenic Microbes", Biology, 12(5), 661, 2023. https://doi.org/10.3390/biology12050661

[88] Urnukhsaikhan, E., Bold, B.-E., Gunbileg, A., Sukhbaatar, N., Mishig-Ochir, T. "Antibacterial activity and characteristics of silver nanoparticles biosynthesized from *Carduus crispus*", Scientific Reports, 11(1), 21047, 2021. https://doi.org/10.1038/s41598-021-00520-2

[89] Dakal, T. C., Kumar, A., Majumdar, R. S., Yadav, V. "Mechanistic Basis of Antimicrobial Actions of Silver Nanoparticles", Frontiers in Microbiology, 7, 1831, 2016. https://doi.org/10.3389/fmicb.2016.01831

[90] Loo, Y. Y., Rukayadi, Y., Nor-Khaizura, M.-A.-R., Kuan, C. H., Chieng, B. W., Nishibuchi, M., Radu, S. "*In Vitro* Antimicrobial Activity of Green Synthesized Silver Nanoparticles Against Selected Gram-negative Foodborne Pathogens", Frontiers in Microbiology, 9, 1555, 2018. https://doi.org/10.3389/fmicb.2018.01555

[91] Yin, I. X., Zhang, J., Zhao, I. S., Mei, M. L., Li, Q., Chu, C. H. "The Antibacterial Mechanism of Silver Nanoparticles and Its Application in Dentistry", International Journal of Nanomedicine, 15, pp. 2555–2562, 2020. https://doi.org/10.2147/IJN.S246764

[92] Mussin, J., Giusiano, G. "Biogenic silver nanoparticles as antifungal agents", Frontiers in Chemistry, 10, 1023542, 2022. https://doi.org/10.3389/fchem.2022.1023542

[93] Das, D., Paul, P. "Plant Nano Biology Environmental impact of silver nanoparticles and its sustainable mitigation by novel approach of green chemistry", Plant Nano Biology, 14, 100210, 2025. https://doi.org/10.1016/j.plana.2025.100210